# Coupled Membrane Fluctuations and Protein Mobility in Supported Intermembrane Junctions

**Raghuveer Parthasarathy and Jay T. Groves***

*Department of Chemistry, University of California, Berkeley, California 94720*

*Received: October 7, 2005; In Final Form: February 16, 2006*

Junctions between lipid membranes make possible cell-free explorations of physical mechanisms that can contribute to protein and lipid organization at a variety of biophysical interfaces. Recent studies of mobile antibodies sandwiched between lipid bilayer membranes have shown that strong intermembrane adhesion and protein mobility alone are sufficient to drive inert proteins into micron-scale patterns of dense and sparse zones. Though the length scale of these patterns was suspected to be related to membrane rigidity, a quantitative understanding has so far been unavailable. We introduce data showing radially structured protein patterns that also demonstrate micron-scale organization. We then provide a simple model that relates the spectrum of membrane fluctuations to the observed protein distributions; in brief, only membrane modes that are slow enough to couple to the protein mobility drive intermembrane protein patterns.

The material properties of cellular membranes, including their rigidity and the fluid mobility of their constituent lipids and proteins proteins, define the physical environment at which a great variety of biochemical phenomena occur. At certain intercellular junctions, biochemical signal transduction processes coincide with remarkable spatial rearrangements on the part of the membrane molecules involved.[1−5] The construction of cell-free intermembrane junctions[6−10] may help delineate the role of physical mechanisms in these spatial organizations and may also help develop a general understanding of membrane-based pattern formation that can be applied to the design of new self-assembled materials. An experimental system that we have recently developed,[6] composed of two lipid bilayers with one species of protein sandwiched between them, gives rise to striking patterns in the protein distribution upon intermembrane adhesion (see Figure 1). The structure of these protein patterns, as well as the experimental setup, has been described in detail elsewhere[6] and will be briefly summarized in the next paragraph. In this paper, we present (i) new data showing radially structured protein patterns, and (ii) calculations that relate the mechanical properties of the upper membrane, namely, its fluctuation spectrum, to the length scale of the intermembrane protein organization. Fluids and soft materials provide many examples of spatial and temporal fluctuations selecting particular morphological growth modes.[11] Our data and model suggest that biomembrane junctions can also be governed by fluctuation-driven pattern formation, in which the interplay between membrane fluctuations and protein mobility drives protein organization.

The intermembrane junctions consist of two lipid bilayers and mobile proteins (Figure 1). First, fluorescently labeled anti-biotin antibodies are bound to a supported lipid membrane containing a small fraction (typically 1%) of lipids with biotinylated headgroups. Due to the lipid mobility, the proteins are two-dimensionally mobile, with a diffusion coefficient $D \approx 1\ \mu m^2/s$. The proteins are uniformly distributed and "inert," with no measurable tendency for aggregation. A giant lipid vesicle, tens of microns in diameter, is introduced into the aqueous environment. It typically ruptures when contacting the

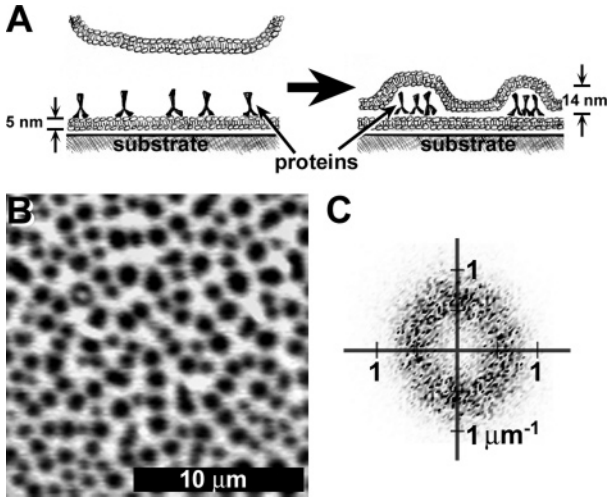


**Figure 1.** Intermembrane protein patterns. (A) Schematic illustration. As described in ref 6, two-dimensionally mobile antibodies are bound to a supported lipid bilayer. Formation of a bilayer−bilayer junction upon the introduction of a second membrane drives the proteins into micron-scale patterns of dense and sparse zones, driven by the bilayer−bilayer adhesion. (B) A fluorescence image of proteins at an intermembrane junction. (The plane defined by the supported membrane is parallel to the page.) Bright regions indicate high protein concentration; dark regions indicate an absence of proteins and tight bilayer−bilayer adhesion. (C) Two-dimensional power spectrum of the protein fluorescence image from the junction of image (B), revealing the few-micron length-scale of the protein pattern.

"lower" membrane and proteins, adhering to the lower membrane to form an intermembrane junction. The "upper" membrane contains no biotinylated lipids; the proteins are bound to the lower membrane only. The rupture and junction formation are rapid, occurring within the temporal resolution of about 0.1 s. Adhesion of the two lipid bilayers drives the mobile proteins into dense zones, clearing them from zones of tight intermembrane contact. A variety of imaging tools, especially interferometric techniques, show that the bilayer−bilayer separation is a few nm in regions of tight contact, and 14 nm in regions where the bilayers are kept apart by the proteins, corresponding to the

10.1021/jp055730d CCC: $33.50 
Published on Web 03/29/2006

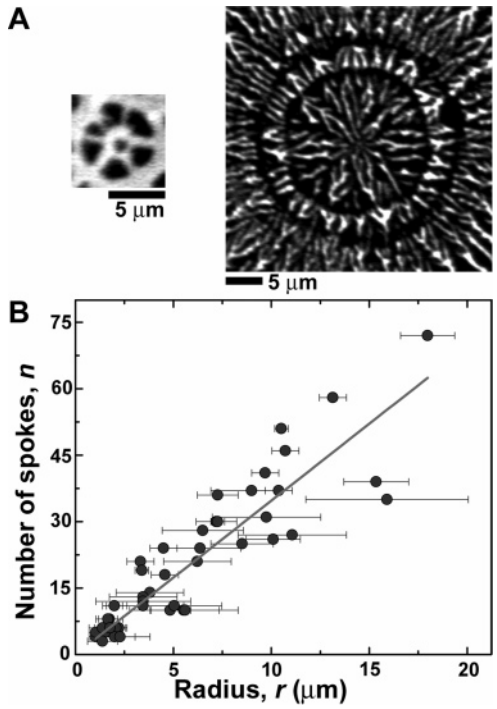


**Figure 2.** Radial intermembrane protein patterns. (A) Fluorescence images of anisotropic intermembrane protein patterns: radial spokes emanating from a central origin. (B) The number of spokes ($n$) plotted as a function of the mean spoke radius ($r$) for 45 sets of radial patterns. The horizontal bars correspond to the radial span of the spokes. The data are consistent with a linear relation between $n$ and $r$; the proportionality reveals a characteristic length scale ($\approx 2$ $\mu$m) identical to that of the isotropic patterns.

size of the antibody molecules oriented as illustrated in Figure 1. Intermembrane adhesion is short-range; the equilibrium intermembrane spacing is a few nm, and the (mostly van der Waals) interaction decays within a few nm of separation.[12,13] The magnitude of the adhesion between membranes is $E_a \approx 0.1$ mJ/m$^2$;[12] over the $A = 30$ nm$^2$ surface area spanned by the proteins, the adhesion energy is nearly 1 $k_BT$, where $k_B$ is Boltzmann's constant and $T$ is the absolute temperature. Adhesion pushes the proteins into locally dense zones, forming zones of tight bilayer−bilayer contact. Since sparse protein zones are seeded by initial intermembrane contact, and proteins are pushed into the surrounding areas until reaching a maximal density, the protein patterns often, though not always, consist of "leopard-spot"-like patterns of disconnected sparse protein zones amid connected dense protein zones (e.g., Figure 1B). Adhesion is so strong that these patterns are kinetically trapped and cannot coarsen (e.g., into one protein-rich and one-protein sparse zone). The characteristic length scale of the leopard-spot patterns of dense and sparse zones is 1−4 $\mu$m (Figure 1). We have noted[6] that this lateral scale is likely to be related to height fluctuations of the upper membrane, but there have to date been no quantitative assessments of this relationship.

In addition to the isotropic leopard-spot protein patterns, a small fraction of intermembrane junctions (roughly 10% of over 400 junctions examined) show radial patterns in the protein distributions − spokes emanating from a central origin (Figure 2). The origin corresponds to the site of initial intermembrane contact. Plotting the number of spokes ($n$) versus the radius (distance from the origin, $r$) for 45 data sets shows a linear relation between $n$ and $r$, and a characteristic length-scale $\xi$ given by $n = 2\pi r/\xi$ (Figure 2). We find $\xi = 1.7 \pm 0.1$ $\mu$m; i.e., the same characteristic scale demonstrated by the isotropic protein patterns. (Calculating $\xi = 2\pi r/n$ for each data point rather than relying on the linear fit between $n$ and $r$ gives an average $\xi = 1.9 \pm 0.7$ $\mu$m, again equal to the isotropic pattern length scale.)

The equivalence of length-scale for the isotropic and radial protein patterns suggests a robust mechanism insensitive to the details of the intermembrane junction formation. This mechanism, we suggest, is connected to the coupling between the rigidity of the upper membrane and the mobility of the intermembrane proteins. The upper lipid membrane is flexible, and is host to a spectrum of fluctuation modes whose frequency ($\omega$) is a function of wavelength ($\lambda$). As the two membranes adhere, only modes that are slow enough to drive the proteins over a distance $\lambda$ in time $\omega^{-1}$ can couple to the protein reorganization. Faster modes, unable to push the membrane-bound proteins aside, will be unable to reach the few-nm intermembrane separation needed for adhesion to the supported bilayer.

Though the rapidity of junction formation precludes direct observation of its fluctuations, recent interferometric experiments on quasi-static intermembrane junctions,[14,15] as well as theoretical studies,[16−19] reveal the dynamics of thermally driven membrane undulations and the influence of the nearby substrate on the fluctuation spectrum. For free membranes,

$$\omega(q) = \frac{\kappa q^3}{4\eta} \tag{1}$$

where $q = 2\pi/\lambda$, $\kappa$ is the bilayer bending rigidity ($\approx 10^{-19}$ J), and $\eta$ is the viscosity of water ($\approx 10^{-3}$ Ns/m$^2$). The presence of a nearby substrate (at distance $z$) slows fluctuations due to the high impedance of fluid flow:

$$\omega(q) = \frac{z^3 \kappa q^6}{12\eta} \tag{2}$$

for $zq \ll 1$ (valid for our experiments). In general, the fluctuation time scale may also be affected by any confinement potential ($V$) experienced by the membrane;[17,20] a term including the second derivative of $V$ with respect to membrane height enters the expression for $\omega$. At the intermembrane separations relevant to our experiments, $z$ ($\approx 10-1000$ nm) is much greater than the equilibrium spacing of a few nm; the interaction potential is nearly flat as a function of distance,[12,13] and the confinement term is negligible.

The protein mobility ($b$) is related to the measured diffusion coefficient ($D$) via the Stokes−Einstein relation. The force ($F$) driving each protein is related to the intermembrane adhesion potential. Consider two membranes, tightly adherent over some range that borders either a single protein or the edge of a cluster of proteins. Protein motion along the membrane plane allows the adhesion zone to grow, and is energetically favorable by an amount corresponding to the difference in adhesion for membranes separated by the protein height compared to tightly adhered membranes: $E_a \approx 0.1$ mJ/m$^2$, as noted above, multiplied by the contact area, $A_C = Lx$, where $x$ is the protein position along the direction of motion, and $L$ is the extent of contact in the perpendicular direction. The force acting on a protein, therefore, is the gradient of the intermembrane adhesion energy with respect to protein position: $F = \mathrm{d}(E_a A_C)/\mathrm{d}x$. Considering the force per protein, using $L \approx \sqrt{A}$, where $A$ is the protein area, we find $F \approx E_a\sqrt{A} \approx 1$ pN. Together, $F$ and $b$ give a protein velocity $v = bF \approx 300$ $\mu$m/s, and a time scale for motion over length $\lambda$ of $\tau_p = \lambda/v$.

Coupling of the protein motion to the membrane fluctuations requires $\tau_p < \omega(q)^{-1}$, or $\lambda > \lambda_c$, where

$$\lambda_c = \left(\frac{2\pi^3\kappa}{\eta v}\right)^{1/2} \quad (3)$$

treating the upper membrane as free, or

$$\lambda_c = \left(\frac{16\pi^6\kappa z^3}{3\eta v}\right)^{1/5} \quad (4)$$

accounting for the damping effect of the substrate. As the upper membrane falls, its separation from the proteins and lower membrane drops from $z \approx 1$ $\mu$m to $z \approx 10$ nm (the final scale being set by the protein height). It is at present unclear which $z$ value dominates the membrane response, as junction formation occurs within our temporal resolution of about 100 ms, preventing monitoring of $z$ − but in determining $\lambda_c$ this uncertainty is unimportant. For $z$ between 10 nm and 1 micron (an effectively free membrane), $\lambda_c$ lies in the range 0.3−4 microns. The time scale of the fluctuation modes slows sharply with increasing wavelength, so modes near $\lambda_c$ rapidly determine the structure of the protein reorganization. Given the simplicity of this model, the agreement between $\lambda_c$ and the observed protein pattern structure ($\xi \approx 1-4$ $\mu$m) is surprisingly good.

Our model (eq 4) suggests weak dependences of the protein pattern length scale on the membrane stiffness ($\lambda_c \sim k^{1/5}$), solution viscosity ($\lambda_A \sim h^{-1/5}$), and protein velocity ($\lambda_c \sim v^{-1/5}$). While conceptually simple, significant modifications of these parameters are experimentally beyond the range of present experimental techniques.

Significantly increasing membrane rigidity while maintaining membrane fluidity is a challenge. Cholesterol, for example, modulates membrane stiffness, but cholesterol-rich membranes readily phase separate into chemically distinct regions. Furthermore, our recent observations (in a manuscript presently under review) reveal connections between phase separation and membrane topography which would complicate the use of such complex membranes in studies of intermembrane pattern formation.

Probing the viscosity dependence of the model requires forming intermembrane junctions under conditions of high viscosity and then characterizing the patterns. Despite repeated attempts, we are unable to form intermembrane junctions in high-viscosity solutions. The upper membranes of the junctions are formed from ruptured giant vesicles, as noted above. In aqueous glycerol solutions (viscosity 3−10 times that of water), we find that the giant vesicles do not rupture. We suspect that this is due to the rupture process itself being sensitive to the membrane fluctuation spectrum: rupture requires an intial, energetically costly, formation of a hole in a continuous membrane. If membrane fluctuations are damped at high viscosity, the hole is prevented. Counteracting the effects of viscosity may be possible by increasing the strength of the intermembrane adhesion, e.g., via charged lipids. However, as the length scale of the protein patterns depends also on adhesion energy (through $v$), this would not provide a clear test of the viscosity dependence of the model.

As for the protein velocity dependence of $\lambda_c$, we note that streptavidin sandwiched between membranes forms similar micron-scale patterns as do antibodies (Figure 3). Streptavidin is less than half the size of the antibodies,[6] and has a tendency to crystallize on membranes,[21] possibly related to an observed high incidence of compact dense, rather than sparse, protein zones (i.e., "inverse leopard-spot" patterns, Figure 3A). Despite these differences with antibodies, it shares the characteristic of attaching to the supported membrane with two biotin-binding sites, and so has a similar mobility. The shared few-micron length scale of streptavidin and antibody patterns (Figures 1C, 3B), therefore, is consistent with our model. Proteins that bind membranes with high affinity and span a range of binding valencies, and hence a range of mobilities, are not readily available. They could, however, be created in future work by using fragments or cross-linked multimers of proteins. Surmounting the technological challenges outlined above should allow further tests of our model. In addition, high-speed interferometric imaging, which should soon be viable, may provide direct observations of the coupling between membrane fluctuation modes[15] and protein motions.

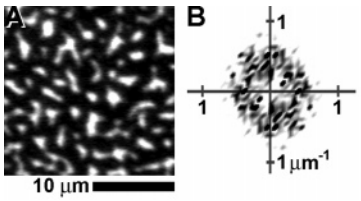


**Figure 3.** Streptavidin, bound to the lower membrane and sandwiched at an intermembrane junction, forms similar spatial patterns as those formed by antibodies. (A) A fluorescence image of streptavidin at an intermembrane junction. (B) Two-dimensional power spectrum of the protein fluorescence image from the junction of image (A), revealing the few-micron length-scale of the protein pattern.

The initial conditions of the junction formation that lead to radial versus isotropic protein patterns are at present unknown, and are likely to depend on subtle differences in the early stages of intermembrane adhesion. Radial instabilities and patterns are common in a variety of membrane, fluid, and thin film systems. Two classes of phenomena especially show a superficial similarity to these radial protein patterns and are worth noting. The collapsing surface of a viscous bubble can demonstrate a radial rippling instability,[22,23] with the number of ripples increasing as a function of the radius of a central puncture.[23] The ripple length-scale is set by a competition between the film's rigidity and a long-range force (gravity). In our membrane systems, there is no energetically significant long-range interaction; gravitational energy is negligible over the small system sizes, and the intermembrane adhesion, as noted earlier, is limited to a few nanometers in range. The radial protein patterns are also reminiscent of instabilities in intermembrane adhesion fronts recently examined experimentally[24] and theoretically.[25] In these systems, the emergent fingering instability is a consequence of the mobility of adhesive elements that bind the membranes. The adhesion between lipid bilayers in our experiments is not mediated by mobile adhesive elements (the mobile antibodies do not contribute to intermembrane adhesion), and so is not subject to this sort of instability.

Protein patterns driven by intermembrane adhesion provide a striking example of the link between protein organization and membrane mechanics. Even inert proteins that neither mediate intermembrane adhesion nor interact with one another can be guided into striking micron-scale patterns simply by virtue of their mobility and their steric couplings to membrane undulations. The behavior of an enormous variety of material systems is governed by particular fluctuation modes dominating morphological evolution; the break-up of a column of water into droplets is one familiar example. As described above, the structure of our intermembrane junctions is set by certain membrane fluctuation modes coupling to the motion of membrane-bound proteins. More generally, these junctions share with other fluid and soft material systems the physical characteristics

that make such self-assembled pattern formation possible: they are strongly driven, are dominated by kinetics rather than equilibrium thermodynamics, and are host to a spectrum of random fluctuations (here provided by thermal energy).[11] The simplicity of composition of lipid membrane junctions makes possible a clear understanding of their dynamics that will serve as a springboard to biophysical studies in more sophisticated contexts, including systems incorporating specific adhesion proteins, multiple protein species, and self-assembled protein complexes. We expect these and other adhesion-driven biomembrane systems, both in vitro and in vivo, to display still further examples of nonequilibrium pattern formation.

**Acknowledgment.** We thank Yoshihisa Kaizuka for helpful discussions, Paul Cripe for experimental assistance, and Nir Gov for first suggesting a quantitative connection between membrane fluctuations and protein mobility during several illuminating discussions. This work was supported by the National Institutes of Health (Grant no. 1 R01 GM64900-01), by the Director, Office of Science, Office of Basic Energy Sciences, Division of Materials Sciences and Engineering, of the U.S. Department of Energy under Contract No. DE-AC03-76SF00098, by a fellowship from the Miller Institute for Basic Research (to R.P.), and by a Beckmann Foundation Young Investigator Award (to J.T.G.).

## References and Notes

(1) Grakoui, A.; Bromley, S. K.; Sumen, C.; Davis, M. M.; Shaw, A. S.; Allen, P. M.; Dustin, M. L. *Science* **1999**, *285*, 221−227.

(2) Davis, D. M.; Chiu, I.; Fassett, M.; Cohen, G. B.; Mandelboim, O.; Strominger, J. L. *Proc. Natl. Acad. Sci. U.S.A.* **1999**, *96*, 15062−15067.

(3) Qi, S. Y.; Groves, J. T.; Chakraborty, A. K. *Proc. Natl. Acad. Sci. U.S.A.* **2001**, *98*, 6548−6553.

(4) Dustin, M. L.; Colman, D. R. *Science* **2002**, *298*, 785−789.

(5) Igakura, T.; Stinchcombe, J. C.; Goon, P. K.; Taylor, G. P.; Weber, J. N.; Griffiths, G. M.; Tanaka, Y.; Osame, M.; Bangham, C. R. *Science* **2003**, *299*, 1713−1716.

(6) Parthasarathy, R.; Groves, J. T. *Proc. Natl. Acad. Sci. U.S.A.* **2004**, *101*, 12798−12803.

(7) Bruinsma, R.; Behrisch, A.; Sackmann, E. *Phys. Rev. E.* **2000**, *61*, 4253−4267.

(8) Kloboucek, A.; Behrisch, A.; Faix, J.; Sackmann, E. *Biophys. J.* **1999**, *77*, 2311−2328.

(9) Albersdorfer, A.; Feder, T.; Sackmann, E. *Biophys. J.* **1997**, *73*, 245−257.

(10) Parthasarathy, R.; Jackson, B. L.; Lowery, T. J.; Wong, A. P.; Groves, J. T. *J. Phys. Chem. B* **2004**, *108*, 649−657.

(11) Ball, P. *The Self-made Tapestry: Pattern Formation in Nature*; Oxford: New York, 1999.

(12) Marra, J.; Israelachvili, J. *Biochemistry* **1985**, *24*, 4608−4618.

(13) Israelachvili, J. *Intermolecular and Surface Forces*, 2nd ed.; Academic Press: New York, 1991.

(14) Kaizuka, Y.; Groves, J. T. *Biophys. J.* **2004**, *86*, 905−912.

(15) Kaizuka, Y.; Groves, J. T. *Phys. Rev. Lett.* **2006**, *96*, 118101.

(16) Prost, J.; Manneville, J. B.; Bruinsma, R. *Eur. Phys. J. B* **1998**, *1*, 465−480.

(17) Gov, N.; Zilman, A. G.; Safran, S. *Phys. Rev. Lett.* **2003**, *90*, 228101.

(18) Brochard, F.; Lennon, J. F. *J. Phys. (Paris)* **1975**, *36*, 1035−1047.

(19) Seifert, U. *Phys. Rev. E* **1994**, *49*, 3124−3127.

(20) Rädler, J. O.; Feder, T. J.; Strey, H. H.; Sackmann, E. *Phys. Rev. E* **1995**, *51*, 4526−4536.

(21) Ratanabanangkoon, P.; Gropper, M.; Merkel, R.; Sackmann, E.; Gast, A. P. *Langmuir* **2002**, *18*, 4270−4276.

(22) Debrègeas, G.; de Gennes, P.; Brochard-Wyart, F. *Science* **1998**, *279*, 1704−1707.

(23) da Silveira, R.; Chaieb, S.; Mahadevan, L. *Science* **2000**, *287*, 1468−1471.

(24) Boulbitch, A.; Guttenberg, Z.; Sackmann, E. *Biophys. J.* **2001**, *81*, 2743−2751.

(25) Shenoy, V. B.; Freund, L. B. *Proc. Natl. Acad. Sci. U.S.A.* **2005**, *102*, 3213−3218.